

## Supporting Information

### **Si-modified Mn-Ce oxide catalyst for selective catalytic reduction of NO<sub>x</sub> with NH<sub>3</sub> at low temperature**

Shuai Wang <sup>a</sup>, Na Zhu <sup>a\*</sup>, Pengpeng Xu <sup>a</sup>, Shuai Li <sup>a</sup>, Di Chen <sup>b</sup>

<sup>a</sup> School of Advanced Manufacturing, Fuzhou University, Jinjiang, 362251, PR China

<sup>b</sup> Smart Devices and High-end Equipment Lab, Foshan (Southern China) Institute for New Materials, Foshan, 528247, PR China

\*Corresponding author.

Tel: +86 595 82660815

E-mail: nzhu@fzu.edu.cn

### 1.1 Catalytic activity test

The NH<sub>3</sub>-SCR performance of the catalysts was evaluated in a fixed-bed quartz reactor. The catalyst samples (40-60 mesh) were put into a quartz tube with an inner diameter of 6 mm, which was placed in a tube furnace, and the temperature was controlled at 50 to 300 °C. The simulated flue gas was composed of 500 ppm NO, 500 ppm NH<sub>3</sub>, 50 ppm SO<sub>2</sub> (when used), 5% O<sub>2</sub> and N<sub>2</sub> balance. The total flow rate was 500 mL·min<sup>-1</sup>, and the corresponding gas hourly space velocity (GHSV) was 5×10<sup>4</sup> h<sup>-1</sup>. The effluent gases, including NH<sub>3</sub>, NO, N<sub>2</sub>O and NO<sub>2</sub>, were analyzed by a Nicolet IS50 FTIR gas analyzer. Activity data were collected when the catalytic reaction actually reached steady-state conditions at each temperature.

### 1.2 Catalyst Characterization

The specific surface area and pore characteristics of the samples were measured by N<sub>2</sub> adsorption/desorption analysis on a physisorption analyzer (MicrotracBEL). The samples need to be degassed at 300 °C for 1 h before N<sub>2</sub> physisorption at 77 K.

X-ray diffraction (XRD) patterns of the samples were recorded on a diffractometer (Bruker D8 Advance, Germany) with CuKα radiation ( $\lambda = 0.154056$  nm) in a  $2\theta$  of 10°–80° at 0.02 °s<sup>-1</sup>.

The temperature programmed desorption of NH<sub>3</sub> (NH<sub>3</sub>-TPD) was carried out on an FTIR spectrometer (Nicolet IS50). The catalyst sample (50 mg) was first pretreated in air at 300 °C for 0.5 h, and then cooled down to 50 °C under N<sub>2</sub> conditions. Afterwards, the catalyst sample was exposed to 500 ppm NH<sub>3</sub>/N<sub>2</sub> until saturation, followed by N<sub>2</sub> purging for 0.5 h. Finally, the catalyst sample was heated from 50 °C to 650 °C in a N<sub>2</sub> flow (100 mL·min<sup>-1</sup>

<sup>1</sup>) at a constant heating rate ( $10\text{ }^{\circ}\text{C}\cdot\text{min}^{-1}$ ). The concentration of  $\text{NH}_3$  was detected using Nicolet IS50 FTIR spectroscopy.

The  $\text{H}_2$  temperature programmed reduction ( $\text{H}_2$ -TPR) experiments were performed on an Autochem 2920 (Micromeritics) analyzer. The samples (50 mg) were pretreated at  $300\text{ }^{\circ}\text{C}$  in a quartz reactor in a flow of Ar ( $50\text{ mL}\cdot\text{min}^{-1}$ ) for 1 h and cooled down to room temperature. Then, from room temperature to  $800\text{ }^{\circ}\text{C}$ ,  $\text{H}_2$ -TPR was performed in a 10 vol.%  $\text{H}_2/\text{Ar}$  gas flow of  $50\text{ mL}\cdot\text{min}^{-1}$  at a heating rate of  $10\text{ }^{\circ}\text{C}\cdot\text{min}^{-1}$ .

The surface element compositions and chemical states of each catalyst sample were evaluated by an X-ray photoelectron spectroscopy (XPS) analyzer (Axis Ultra, Kratos Analytical Inc.) using Al  $\text{K}\alpha$  X-ray radiation ( $1486.6\text{ eV}$ ). All of the binding energies were calibrated using the C 1s peak (binding energy =  $284.8\text{ eV}$ ) as a standard.

The adsorption behavior of the reactants and their surface reactions were studied by *in situ* diffuse reflectance infrared Fourier transform spectroscopy (*in situ* DRIFTS), which was carried out on a Brooker VERTEX 80/80V Fourier transform infrared spectrometer (Brück, Germany) equipped with liquid nitrogen-cooled MCT detection. The powder sample was pretreated in 20 %  $\text{O}_2/\text{N}_2$  at  $450\text{ }^{\circ}\text{C}$  for 0.5 h prior to adsorption experiments. The following conditions were controlled as follows: 500 ppm  $\text{NH}_3$ , or 500 ppm  $\text{NO} + 5\%$   $\text{O}_2$ ,  $\text{N}_2$  balance, and the total flow rate was kept at  $300\text{ mL}\cdot\text{min}^{-1}$ . For the experiments on  $\text{NH}_3$  or  $\text{NO}_x$  adsorption, the sample was saturated with  $\text{NH}_3/\text{N}_2$  or  $\text{NO}_x/\text{N}_2$  for 40 min, and then purged with  $\text{N}_2$  for 30 min. All spectra were recorded by accumulating 100 scans with a resolution of  $4\text{ cm}^{-1}$ .

### 1.3 Kinetics experiment

In order to obtain a further understanding of the effect of Si doping and sulfation after-treatment on the NH<sub>3</sub>-SCR reaction, the kinetics experiments were studied on Mn<sub>4</sub>Ce<sub>6</sub>, Mn<sub>4</sub>Ce<sub>5</sub>Si<sub>1</sub> and Mn<sub>4</sub>Ce<sub>5</sub>Si<sub>1</sub>-1S% catalysts. The samples with particles of 40-60 mesh and a total gas flow rate of 500 mL·min<sup>-1</sup> were selected to rule out internal and external transfer diffusion. The NO<sub>x</sub> conversion was controlled below 20%. The NO<sub>x</sub> reduction rates (mol·g<sup>-1</sup>·s<sup>-1</sup>) and activation energy (E<sub>a</sub>) were calculated based on the following equations:

$$-r = \frac{F}{W} \ln(1 - x)$$

$$k = \frac{r}{[NO]_0} = A e^{-E_a / RT}$$

where F is the NO<sub>x</sub> flow rate, [NO<sub>x</sub>]<sub>0</sub> is the NO<sub>x</sub> concentration at the inlet, W is the mass of catalyst, E<sub>a</sub> is the apparent activation energy, T is the Kelvin temperature, R is the gas constant (8.314 J/(mol·K)), and A represents the pre-factor.

## 2 Results

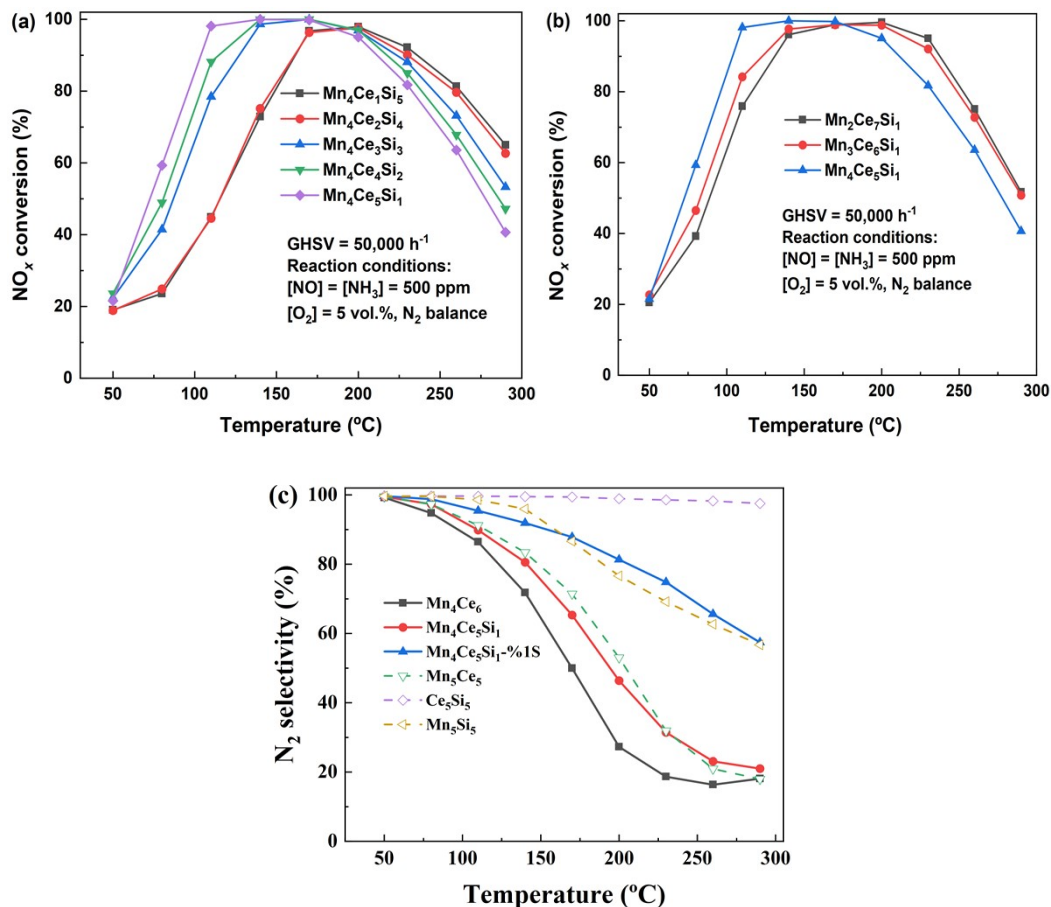


**Fig. S1** NO<sub>x</sub> conversion and N<sub>2</sub> selectivity versus temperature over different catalysts: different Ce/Si molar ratios (a), different Mn/Ce molar ratios (b), and N<sub>2</sub> selectivity (c).

A series of Si-modified Mn-Ce oxide catalysts were prepared to study the effect of the Si element on the NH<sub>3</sub>-SCR activity of Mn-Ce oxide catalysts, as shown in Fig. S1. When the content of Mn was constant, the increase of Si/Ce ratio resulted in a decrease in NO<sub>x</sub> conversion at low temperature. However, the catalyst activity (>200 °C) was in the order following: Mn<sub>4</sub>Ce<sub>1</sub>Si<sub>5</sub> > Mn<sub>4</sub>Ce<sub>2</sub>Si<sub>4</sub> > Mn<sub>4</sub>Ce<sub>3</sub>Si<sub>3</sub> > Mn<sub>4</sub>Ce<sub>4</sub>Si<sub>2</sub> > Mn<sub>4</sub>Ce<sub>5</sub>Si<sub>1</sub>. The Mn<sub>a</sub>Ce<sub>b</sub>Si<sub>c</sub> with different Mn/Ce ratios was also investigated, and the Mn<sub>4</sub>Ce<sub>5</sub>Si<sub>1</sub> catalyst showed the widest temperature window and highest NO<sub>x</sub> conversion (> 90%) at 100-260 °C.

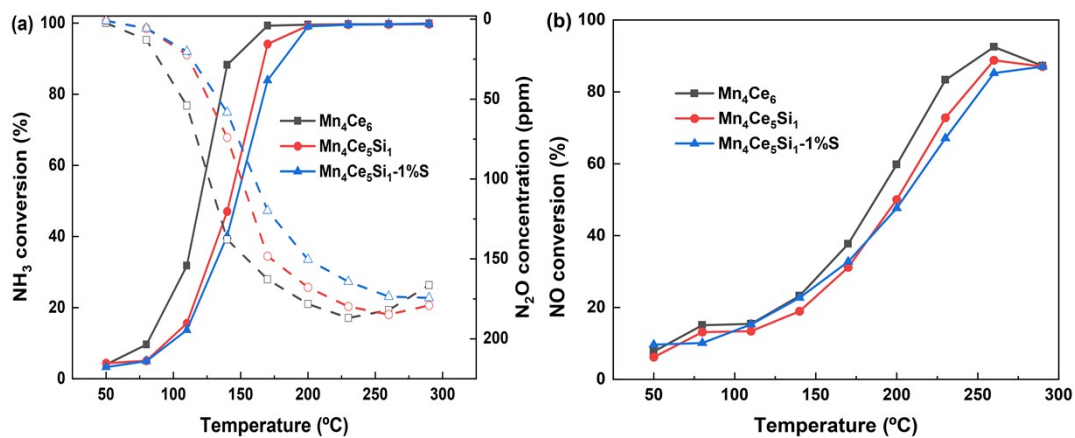


**Fig. S2** (a)  $NH_3$  conversion and (b) NO conversion in separate  $NH_3$  and NO oxidation reactions over  $Mn_4Ce_6$ ,  $Mn_4Ce_5Si_1$  and  $Mn_4Ce_5Si_1-1\%S$ .

As shown in Fig. S2, the  $Mn_4Ce_6$  catalyst showed the best  $NH_3$  oxidation activity and NO oxidation activity. The introduction of Si resulted in the decrease of activation of  $NH_3$  and NO, which is the reason of the enhanced  $N_2$  selectivity and decreased catalytic activity at low temperature.

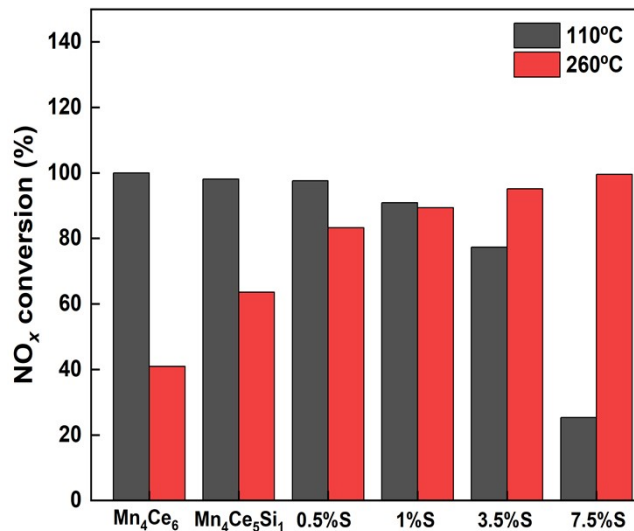


**Fig. S3** NO<sub>x</sub> conversion of catalysts with different H<sub>2</sub>SO<sub>4</sub> loadings at 260 and 110 °C.

Mn<sub>4</sub>Ce<sub>5</sub>Si<sub>1</sub> was sulfation after-treated with varying concentrations of sulfuric acid solution, and the NO<sub>x</sub> conversions at 110 °C and 260 °C of catalysts are shown in Fig. S3. With the increase in sulfuric acid concentration, the NO<sub>x</sub> conversion at 110 °C decreased and the NO<sub>x</sub> conversion at 260 °C increased over Mn<sub>4</sub>Ce<sub>5</sub>Si<sub>1</sub>-x%S catalysts. When the loading amount of sulfuric acid was 1%, the Mn<sub>4</sub>Ce<sub>5</sub>Si<sub>1</sub>-1%S catalyst showed a high NO<sub>x</sub> conversion above 90% in the range of 110-260 °C.

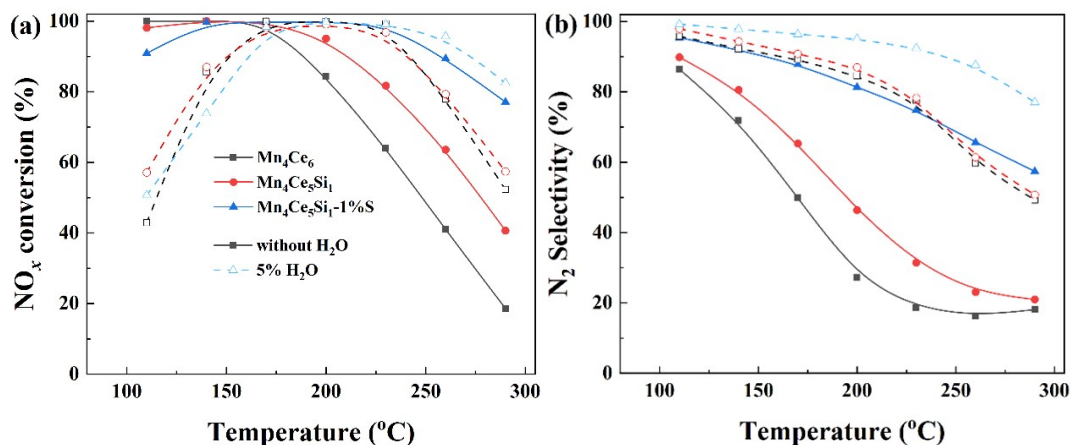


**Fig. S4** Effect of H<sub>2</sub>O on the performance of catalyst.

As shown in Fig. S4, when 5% H<sub>2</sub>O was added to the reaction gas, the NO<sub>x</sub> conversion of all the catalysts decreased below 170°C due to the competitive adsorption of H<sub>2</sub>O, while that increased above 170°C, which may be attributed to the inhibition of the unselective oxidation of NH<sub>3</sub> at high temperature. The N<sub>2</sub> selectivity of all the catalysts was enhanced significantly at the present of H<sub>2</sub>O (Fig. S4b). In comparison, the H<sub>2</sub>O tolerance of Mn-Ce oxide catalysts was improved after Si modification and sulfation after-treatment.



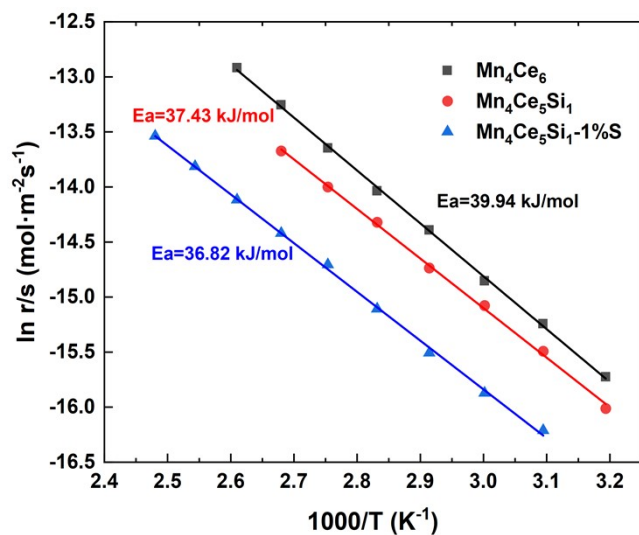


**Fig. S5** NO<sub>x</sub> reduction rates as a function of reaction temperature over Mn<sub>4</sub>Ce<sub>6</sub>, Mn<sub>4</sub>Ce<sub>5</sub>Si<sub>1</sub> and Mn<sub>4</sub>Ce<sub>5</sub>Si<sub>1</sub>-1%S catalysts.

To further understand the effect of Si and sulfation after-treatment on the reaction kinetics of NO<sub>x</sub> reduction over Mn-Ce oxide catalysts, Arrhenius plots of the NH<sub>3</sub>-SCR reaction are shown in Fig. S4. It can be seen that Mn<sub>4</sub>Ce<sub>6</sub>, Mn<sub>4</sub>Ce<sub>5</sub>Si<sub>1</sub> and Mn<sub>4</sub>Ce<sub>5</sub>Si<sub>1</sub>-1%S have similar Ea (~37 kJ/mol), indicating of identical catalytic centers and rate-limiting steps.

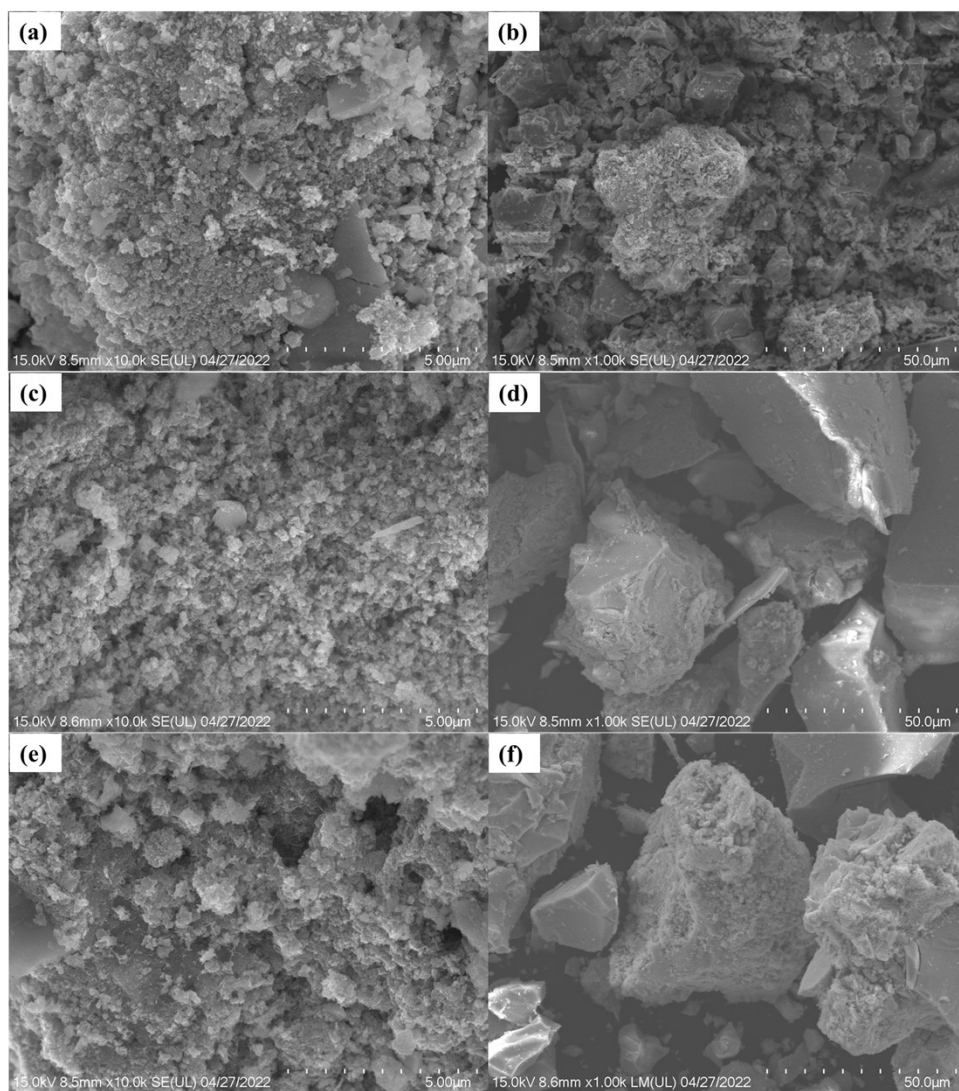


**Fig. S6** SEM images of (a and b)  $Mn_4Ce_6$ , (c and d)  $Mn_4Ce_5Si_1$ , and (e and f)  $Mn_4Ce_5Si_1$ -1%S catalysts.

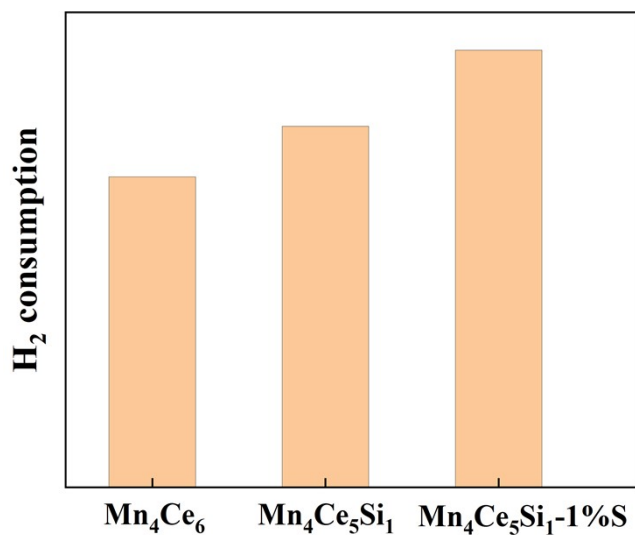


**Fig. S7** H<sub>2</sub> consumption of Mn<sub>4</sub>Ce<sub>6</sub>, Mn<sub>4</sub>Ce<sub>5</sub>Si<sub>1</sub>, and Mn<sub>4</sub>Ce<sub>5</sub>Si<sub>1</sub>-1%S catalysts.

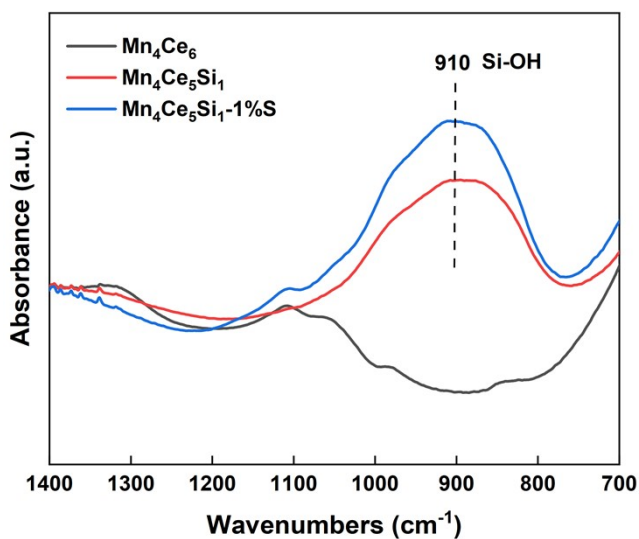


**Fig. S8** FT-IR spectra of Mn<sub>4</sub>Ce<sub>6</sub>, Mn<sub>4</sub>Ce<sub>5</sub>Si<sub>1</sub>, and Mn<sub>4</sub>Ce<sub>5</sub>Si<sub>1</sub>-1%S catalysts.

A distinct band attributed to the Si-OH bond (ca. 910 cm<sup>-1</sup>) was detected on Mn<sub>4</sub>Ce<sub>5</sub>Si<sub>1</sub> and Mn<sub>4</sub>Ce<sub>5</sub>Si<sub>1</sub>-1%S, suggesting the abundant surface hydroxyl groups formed on the catalyst surface after the introduction of Si and sulfation after-treatment.<sup>1</sup>

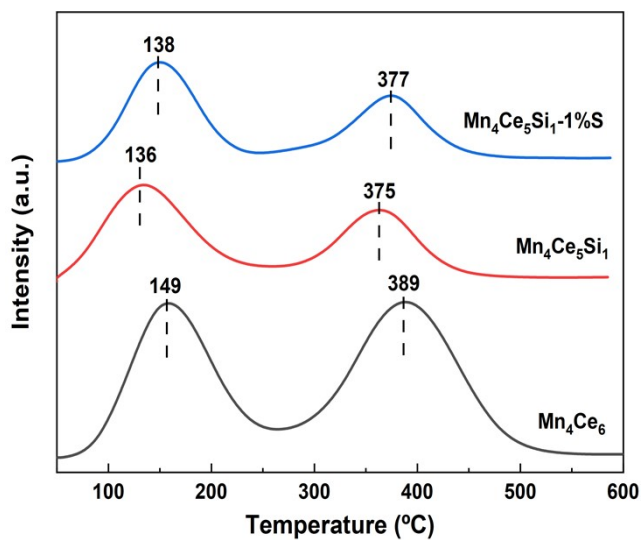


**Fig. S9** NO-TPD profiles of  $\text{Mn}_4\text{Ce}_6$ ,  $\text{Mn}_4\text{Ce}_5\text{Si}_1$  and  $\text{Mn}_4\text{Ce}_5\text{Si}_1\text{-1\%S}$ .

The NO-TPD profiles (Fig. S9) showed two distinct desorption peaks at 136-149 °C and 375-389 °C, which were attributed to physical-absorbed  $\text{NO}_x$  or the decomposition of monodentate nitrate species and the decomposition of bidentate nitrates or bridged nitrate species, respectively.<sup>1</sup>

## References

1. W. Tan, A. Liu, S. Xie, Y. Yan, T. Shaw, Y. Pu, K. Guo, L. Li, S. Yu, F. Gao, F. Liu and L. Dong, *Environ. Sci. Technol.*, 2021, **55**, 4017-4026.